Available online at www.sciencedirect.com
SCIENCE DIRECT®
Journal of Power Sources 142 (2005) 56–69
JOURNAL OF POWER SOURCES
www.elsevier.com/locate/jpowsour

Experimental studies of a direct methanol fuel cell

Jiabin Ge, Hongtan Liu*

Department of Mechanical Engineering, University of Miami, Coral Gables, FL 33146, USA

Received 18 October 2004; accepted 15 November 2004
Available online 5 January 2005

Abstract

Systematic experiments have been conducted to study the effects of various operating parameters on the performances of a direct methanol fuel cell (DMFC). The effects of cell operating temperature, methanol concentration, anode flow rate, air flow rate, and cathode humidification have been studied. The experimental results showed that all the studied operating parameters, except the cathode humidification, have significant effects on the DMFC cell performances, and the cathode humidification has almost negligible effect. The study revealed that the detrimental effect of methanol crossover can be alleviated by increasing cathode air flow rate or oxygen partial pressure. This result showed that the cathode structure and operating condition may play a very important role in DMFC design and operations. The experimental results are presented in both graphical and tabular forms.

Keywords: DMFC; Fuel cell

1. Introduction

Direct methanol fuel cell (DMFC) is considered as a highly promising power source, especially for portable electronics and vehicular applications, due to its important attributes: quick refueling, low temperature and pressure operation, low cost of methanol, no liquid electrolyte, compact cell design, etc. The DMFC technology is a further development of the familiar hydrogen polymer electrolyte membrane fuel cell (PEMFC) technology, and its main drawbacks are low efficiency and low power density, which are caused by methanol permeation through the polymer membrane and slow electrochemical methanol oxidation. Methanol permeation through the polymer membrane reduces fuel utilization and, moreover, is responsible for mixed potential formation at the cathode, which further reduces the efficiency of the cell. Before a break-through in the membrane technology, optimizing design and operating condition for DMFC are critical in improving DMFC performances.

Surampidi et al. [1] studied the effect of temperature and methanol concentration on liquid feed DMFC. The performances were measured at 30, 60, 90 °C, respectively, and the results showed a marked increase in performance with increase in temperature. The methanol concentrations of 0.5, 2.0, and 4.0 M were used; and the results showed the highest voltage was obtained with 2 M methanol concentration when current densities were high, and the optimum concentration was between 0.5 and 2 M methanol. Jung et al. [2] studied the effect of operating temperature (60–120 °C) and methanol concentration (0.5–4.0 M) of a single DMFC. The anode flow rate was 9 ml min^{-1} and pure oxygen at a flow rate of 105 sccm. The results showed the cell performance increased with temperature and an optimal methanol concentration 2.5 M was found at these conditions. Nakagawa and Xiu [3] studied a liquid-feed DMFC with operating temperature ranging from 30–100 °C and the effect of flow rate of oxidant gas (air and oxygen, respectively). In this paper, the results of a systematic experimental study of the effects of various operating parameters on the performance of a DMFC are presented.

* Corresponding author. Tel.: +1 3052842019; fax: +1 3052842580.
E-mail address: hliu@miami.edu (H. Liu).

0378-7753/$ – see front matter © 2004 Elsevier B.V. All rights reserved.
doi:10.1016/j.jpowsour.2004.11.022

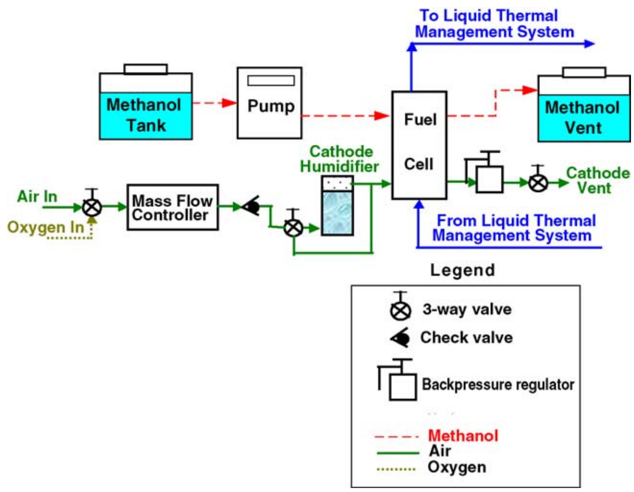

Fig. 1. Schematic of experimental system.

2. Experimental system

The fuel cell test station was manufactured by Fuel Cell Technology, Inc. A major component of the test station is the HP® 6050A system DC electronic load controller, which is capable of controlling the electrical load on the fuel cell as well as measuring its voltage versus current responses. This experimental system also provides control over anode and cathode flow rates, cell operating temperature, operating pressure, and humidification temperature for the cathode. The cathode mass flow is controlled and measured by a MKS® mass flow controller, and the anode flow rate is controlled and measured by a peristaltic pump by Gilson, Inc.

The experimental fuel cell consists of two 316 stainless steel end plates, two graphite collector plates with machined serpentine flow fields, two carbon cloth diffusion layers, two catalyst layers, and the membrane. The cell was kept at a constant temperature during each experiment. The membrane used was Nafion® 117, the gas diffusion layers were carbon cloth, the catalyst was Pt–Ru on the anode side with a loading of 3 mg cm^{-2}, and the catalyst was Pt-black on the cathode side with a loading of 3 mg cm^{-2}. Fig. 1 shows the schematic of the experimental system.

3. Results and discussions

3.1. Effect of cell temperature

A set of experiments were carried out to study the effect of fuel cell temperature in the range of 30–80 °C with an increment of 10 °C. In this set of experiments the cathode inlet temperature was kept at 30 °C, air flow rate was set at 600 sccm, methanol flow rate was 4 ml min^{-1}, and methanol concentration was 3 M. The catalyst loadings were 3 mg cm^{-2} Pt–Ru on the anode side and 3 mg cm^{-2} Pt-Black on the cathode side.

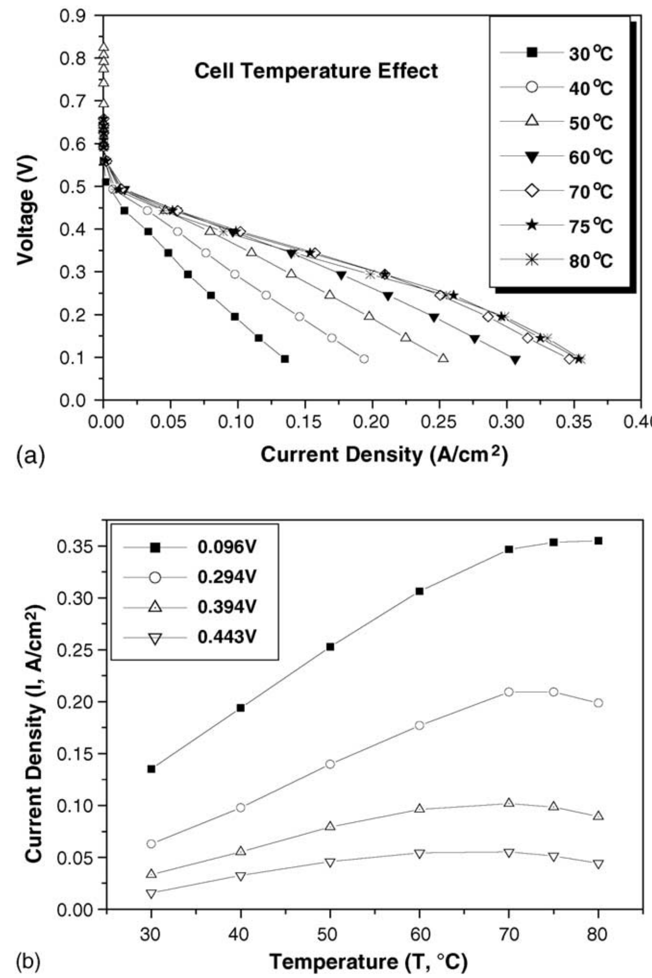

Fig. 2. Experimental results at different fuel cell operating temperatures: methanol concentration, 3 M; cathode humidification temperature, 30 °C; methanol flow rate, 4 ml min^{-1}; air flow rate, 600 sccm. (a) Polarization curves at different temperatures; (b) fuel cell current density as function of fuel cell operating temperature at different cell voltages.

The polarization curves of this experiment are shown in Fig. 2a. It can be seen that current density increases with cell temperature. This is as expected, since both methanol oxidation kinetics and cathode kinetics improve as temperature increases. In order to closely examine the effects of operating temperature, Fig. 2b is produced, where relationships between current density and temperature at different cell voltages are provided. From this figure, it can be seen that the current density is not a monotonous function of temperature, but has a maximum for each cell voltage. It is also clear that the maximum current densities are different at different cell voltages. The maximum current density increases as cell voltage decreases.

On one hand, the electrochemical kinetics on cathode and anode increase with temperature; on the other hand, higher cell temperature also has the following negative effects: (a) the oxygen partial pressure decreases with temperature due to the increase of vapor partial pressure, which causes both decreases in open-cell voltage and increases in concentration overpotential; (b) the rate of methanol crossover increases with temperature [4,5], thus decreases the cell performance; (c) water transfer from anode to cathode through the membrane increases with temperature [7,9], and the additional water increases the liquid water fraction in both the cathode catalyst layer and diffusion layer, thus causes an increase in concentration polarization. The effect of temperature is the resulting effects of both the positive effect of temperature on kinetics and the combined negative effects of temperature. Since the effect of temperature on the kinetics is more significant at lower cell voltage, i.e., at higher current density, it takes greater negative effect of temperature to offset this positive effect. Thus, the positive slope on the curves of current density versus temperature extends to a higher temperature region, and therefore, the maxima increases with decrease in cell voltage.

3.2. *Effect of methanol concentration*

First, two sets of experiments were carried out to study the effects of methanol concentration. For both sets of experiments, the cell temperature was maintained at 70 °C, cathode humidification temperature was also 70 °C, and methanol flow rate was 6 ml min^{-1}. The air flow rate was 600 sccm for the first set of experiments and 1200 sccm for the second set. Seven different methanol concentrations were used for each set of experiments. Figs. 3 and 4 show the results of the two sets of experiments, respectively. It is clear from Fig. 3 that the best concentration is between 1 and 2 M, and the current density decreases sharply with increasing concentration when the methanol concentration is greater than 2 M. This result is consistent with the result reported in the literature (e.g. [6,8]). The higher the concentration is, the more severe the problem of methanol crossover becomes.

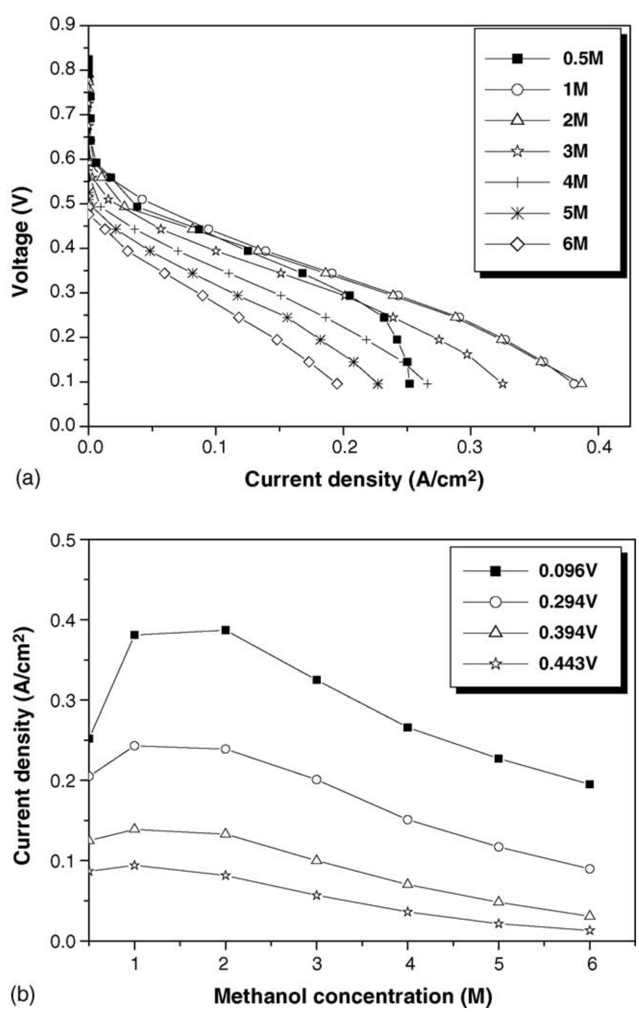

Fig. 3. Experimental results for different methanol concentrations: cell temperature, 70 °C; cathode humidification temperature, 70 °C; methanol flow rate, 6 ml min^{-1}; air flow rate, 600 sccm. (a) Polarization curves; (b) current density vs. methanol concentration at different cell voltages.

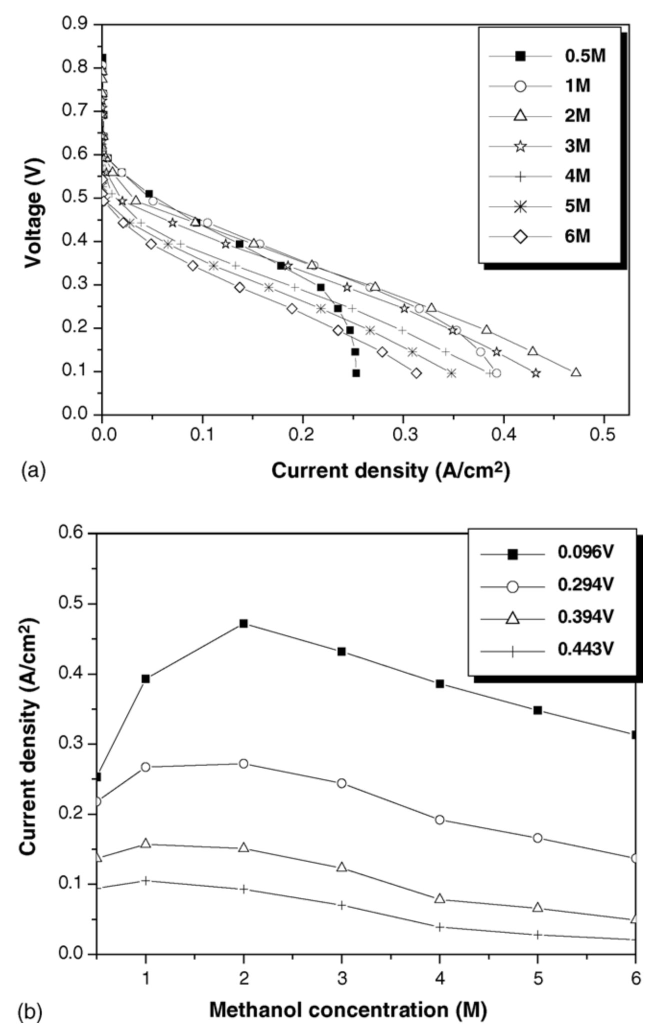

Fig. 4. Experimental results for different methanol concentrations: cell temperature, 70 °C; cathode humidification temperature, 70 °C; methanol flow rate, 6 ml min^{-1}; air flow rate, 1200 sccm. (a) Polarization curves; (b) current density vs. methanol concentration at different cell voltages.

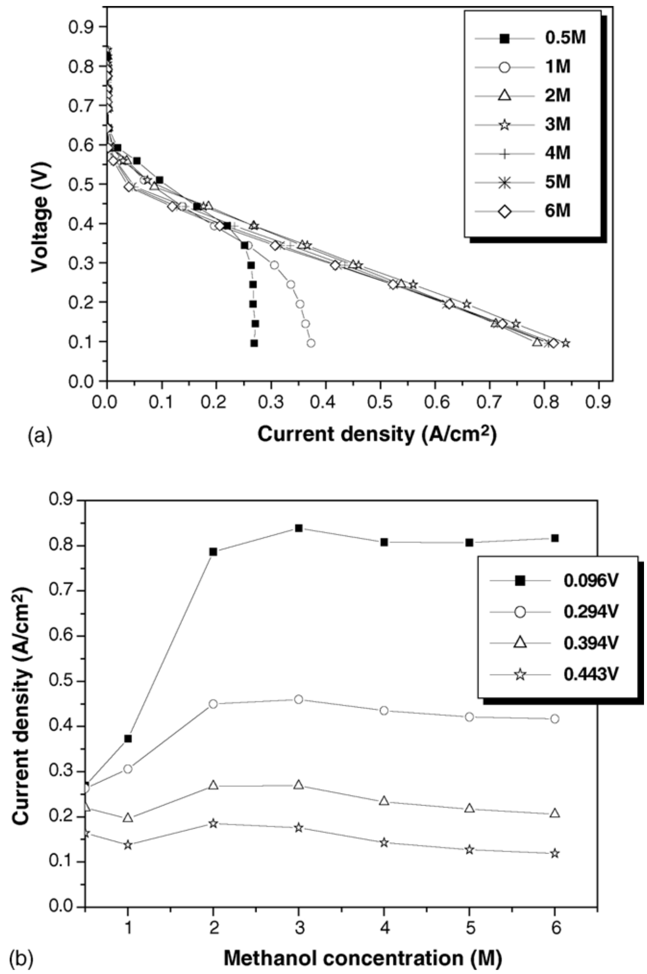

Fig. 5. Experimental results for different methanol concentrations with pure oxygen: cell temperature, 70 °C; cathode humidification temperature, 70 °C; methanol flow rate, 6 ml min^{-1}; pure oxygen flow rate, 600 sccm. (a) Polarization curves; (b) current density vs. methanol concentration at different cell voltages.

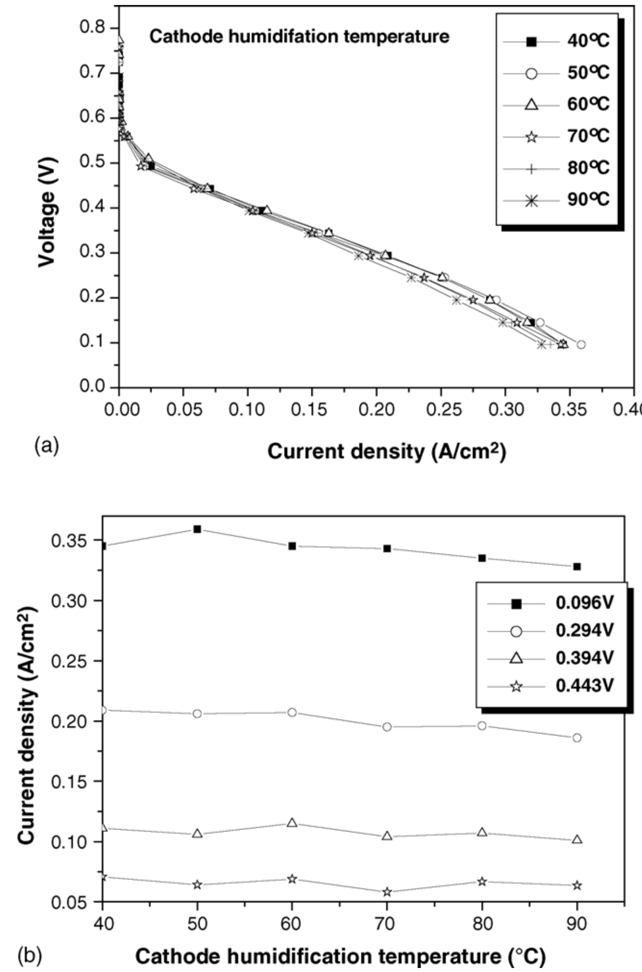

Fig. 6. Experimental results of fuel cell performance at different cathode humidification temperatures: cell temperature, 70 °C; methanol concentration, 2 M; methanol flow rate, 6 ml min^{-1}; air flow rate, 600 sccm. (a) Polarization curves; (b) curve of current density as the function of cathode humidification at different voltage.

The results shown in Fig. 4 are very similar to those in Fig. 3, except that the effect of methanol crossover is not as significant, as indicated by the less steep slopes of the curves in Fig. 4b. Besides, at very low cell voltage, the cell current density is significantly higher at 2 M than that at 1 M. These results indicate that the cathode oxygen supply may play a role in the effect of methanol crossover. It seems that when enough oxygen is supplied to the cathode, the methanol permeated to the cathode side can be oxidized quickly and has a reduced adverse effect on cell performance.

To further investigate the above hypothesis, the third set of experiments was conducted, using pure oxygen at the cathode. If the hypothesis was right, the effect of the methanol crossover would be significantly reduced. Fig. 5 shows the experimental results, which indeed show the anticipated trend. Not only is the adverse effect of higher methanol concentration significantly mitigated, but the optimal methanol concentration also changed from between 1 and 2 M to between 2 and 3 M. These experiments demonstrate that the effects of methanol crossover also depend on the cathode conditions. Further research may find ways to use much higher concentration of methanol solutions. This could significantly reduce the total weight of the fuel carried.

3.3. *Effects of cathode humidification temperature*

Several sets of experiments were conducted to study the effects of cathode humidification temperature. Since all the results are similar, only the results of two sets are shown here in Figs. 6 and 7. In both sets, the cathode humidification temperature was varied from 40–90 °C, the cell temperature was kept at 70 °C, methanol concentration was 2 M and flow rate was 6 ml min^{-1}. The difference is in the cathode flow rate. The cathode flow was 600 sccm for those shown in Fig. 6 and 1200 sccm for those shown in Fig. 7.

Basically, the effect of cathode humidification temperature is not significant. This indicates that de-hydration of the membrane is not a problem in DMFC operations, and no hu-

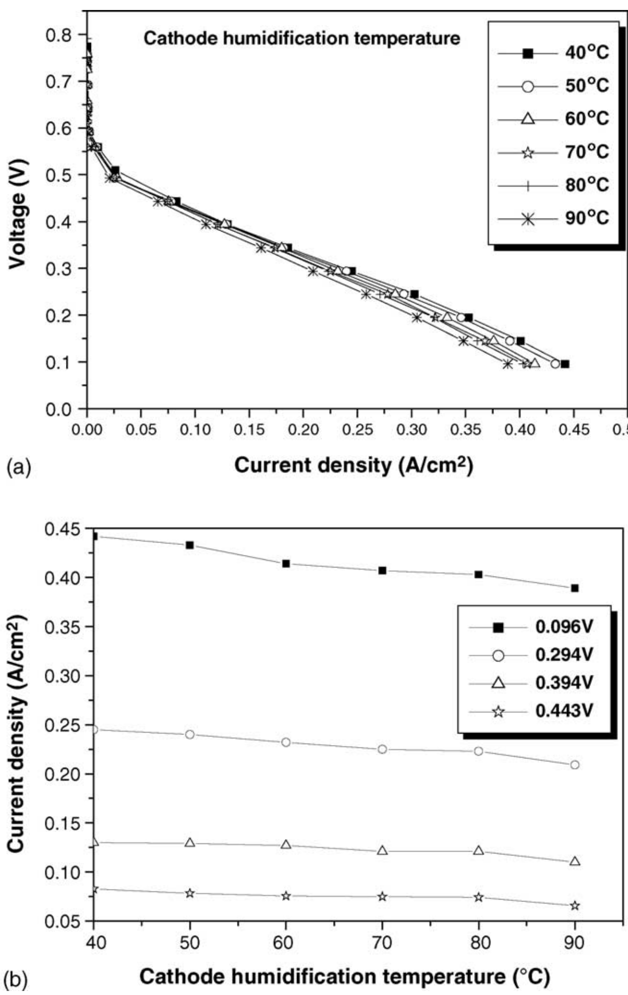

Fig. 7. Experimental results of fuel cell performance at different cathode humidification temperatures: cell temperature, 70 °C; methanol concentration, 2 M; methanol flow rate, 6 ml min^{-1}; air flow rate, 1200 sccm. (a) Polarization curves; (b) current density as the function of cathode humidification at different voltage.

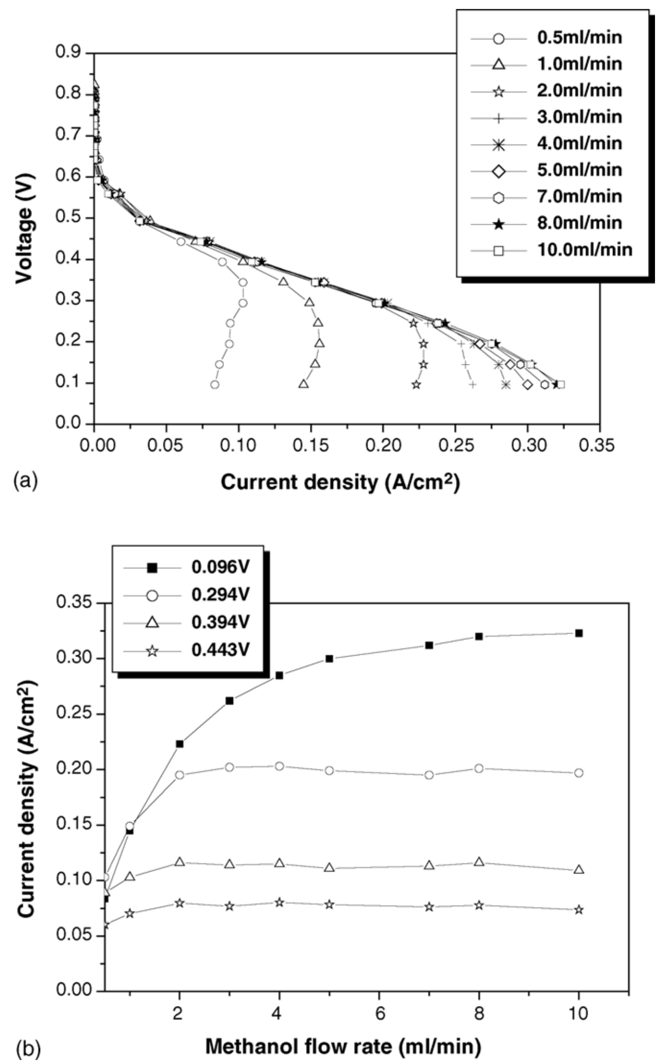

Fig. 8. Experimental results of fuel cell performance at different methanol flow rates: cell temperature, 70 °C; cathode humidification temperature, 70 °C; methanol concentration, 1 M; air flow rate, 1200 sccm. (a) Curves of current density and voltage at different methanol flow rates; (b) curves of current density as the function of methanol flow rate at different voltage.

midification of the cathode stream is necessary. The results further shows that the cell performance decreases with the increase in cathode humidification temperature, especially in the case when the cathode flow rate is high (Fig. 7), which indicates possible minor flooding in the cathode side. On the other hand, this result also shows that flooding is not a significant problem. At such high humidification temperature as 90 °C, with the water production and electro-osmosis effect, there must be significant amount of excess liquid water, but there is no significant decrease in cell performance. Thus, the existence of liquid water in a fuel cell does not necessarily result in flooding.

3.4. Effect of anode flow rate

Figs. 8 and 9 show the results of two sets of experiments for different anode flow rates. The methanol concentration was 1 M, cell temperature was 70 °C, cathode humidification temperature was 70 °C, and air flow rates were 1200 and 600 sccm, respectively. Generally, at a given cell voltage, current density increases with anode flow rate up to certain point, after which anode flow rate has no effects.

An interesting phenomenon can be observed after current density reached the limiting value for all the low flow rate cases. Generally, when a fuel cell reaches its liming current density, no further increase in overpotential (i.e. no further decrease in cell voltage) will change the current density. Here we can clearly observe from both Figs. 8 and 9 that, the current densities decrease as the overpotential further increases (cell voltage decrease) after limiting current densities are reached. Though no conclusive explanations can be provided here, we think this phenomena may be due to that methanol crossover increases with increasing cell overpotential.

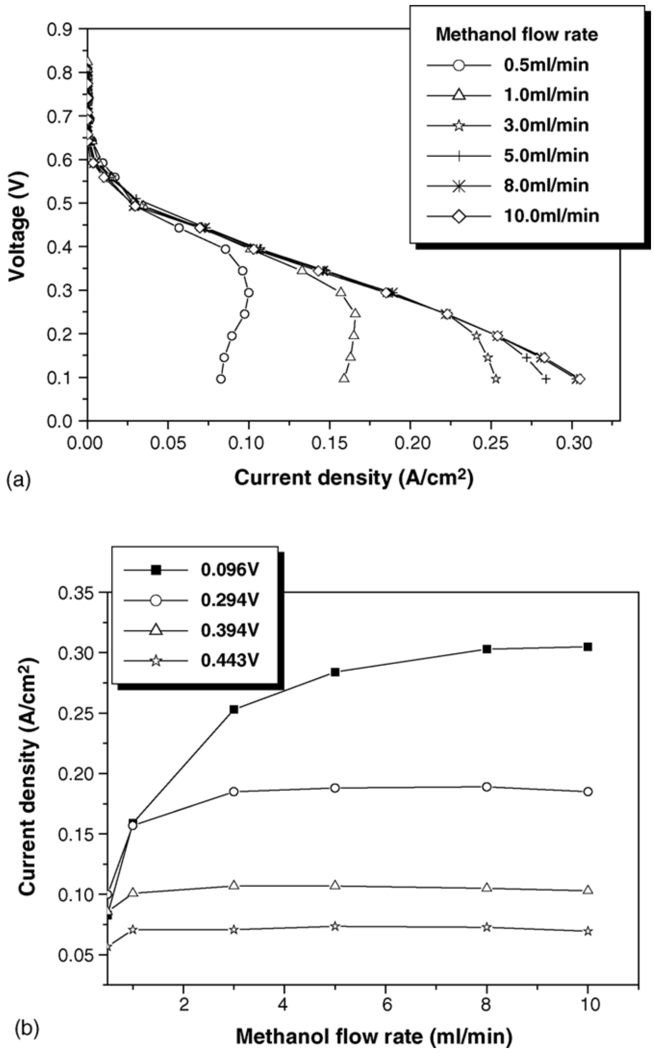

Fig. 9. Experimental results of fuel cell performance at different methanol flow rates: cell temperature, 70 °C; cathode humidification temperature, 70 °C; methanol concentration, 1 M; air flow rate, 600 sccm. (a) Curves of current density and voltage at different methanol flow rates; (b) curves of current density as the function of methanol flow rate at different voltage.

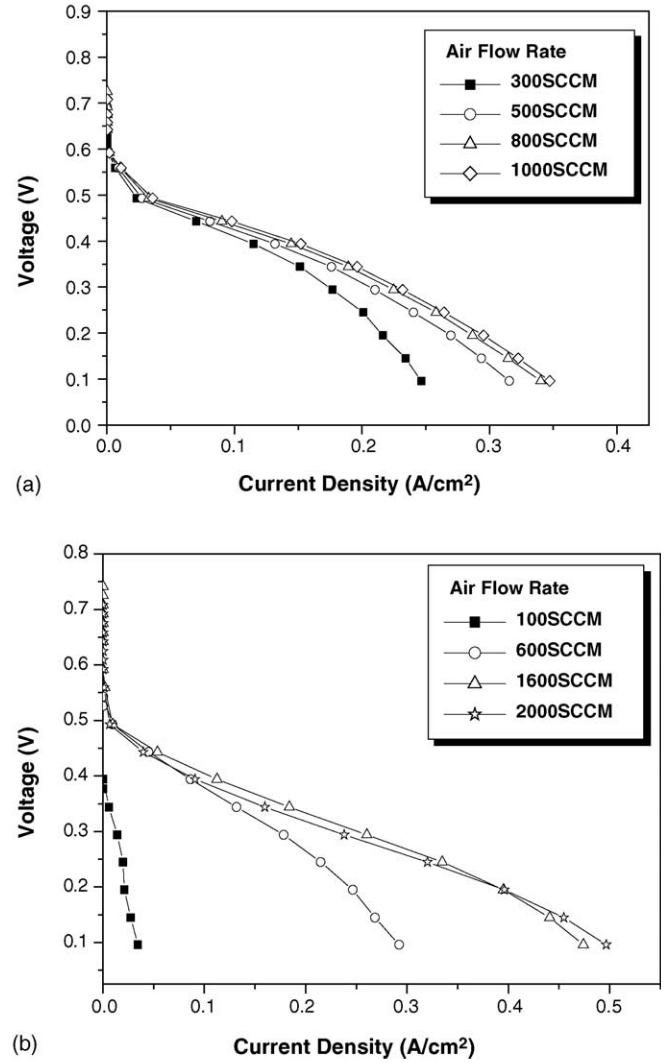

Fig. 10. Comparison of curves of current density and voltage at different air flow rates: methanol concentrations, 2 M (a) and 4 M (b); cell temperature, 75 °C; cathode humidification temperature, 75 °C; methanol flow rates, 5 ml min^{-1} (a) and 4 ml min^{-1} (b).

3.5. *Effect of air flow rate*

Fig. 10 shows the results of effect of air flow rate on cell performance. In Fig. 10a, methanol concentration was 2 M, both cell and cathode humidification temperatures were 75 °C, methanol flow rate was 5 ml min^{-1}.

In Fig. 10b, the methanol concentration was 4 M, both cell and cathode humidification temperatures were 75 °C, and the methanol flow rate was 4 ml min^{-1}. From both Fig. 10a and b, it is clear that the cell performance increase with air flow rate up to a certain value, after which the air flow rate has no significant effect. This result is similar to hydrogen fuel cells and is as expected. With lower air flow rate, oxygen concentration decreases significantly along the flow channels, and results in lower current density. When air flow rate is high enough, any further increase in flow rate will change the oxygen concentration profile only slightly; thus, it has a negligible effect. Additionally, air flow plays a critical role in preventing flooding by removing liquid water from the gas diffusion layer and from the channels.

4. Concluding remarks

The performance of a direct methanol fuel cell under various operating conditions has been carried out to systematically study the effects of operating temperature, methanol concentration, cathode humidification temperature, anode and cathode flow rates. Based on the results of these experiments, the following conclusions can be made:

- Operating temperature has a duel effect on cell performance. Generally the cell performance increases with operating temperature, but up to a point, the adverse effect of temperature may become dominant. Thus a maximum current density exists and this maxima increases as cell voltage decreases.

- For this specific cell design, the optimum methanol concentration is between 1 and 2 M with air as the oxidant, but at a higher air flow rate, the adverse effect of methanol crossover is mitigated. Furthermore, when pure oxygen is used as the oxidant, adverse effect of the methanol crossover is significantly reduced. These results show that proper cathode design and operating condition may enable us to use much higher concentration of methanol, thus significantly reducing the total fuel weight.
- Humidification at the cathode side does not have a significant effect, thus humidification for DMFC is not necessary.
- Anode flow rate has a significant effect on cell performance up to a point, after which further increase in anode flow rate has no effect.
- Generally cell performance increases with air flow rate, but the effect is less pronounced than that of anode flow rate. Similarly, when air flow rate reaches a certain value, any further increase has no significant effects.

Appendix

Table 1
The experimental data of cell performance at different temperatures

$T = 30\,°C$		$T = 40\,°C$		$T = 50\,°C$		$T = 60\,°C$	
V	I (A cm^{-2})	V	I (A cm^{-2})	V	I (A cm^{-2})	V	I (A cm^{-2})
0.609	0.000233	0.609	0.000233	0.824	0.000233	0.642	0.000233
0.609	0.000233	0.609	0.000233	0.807	0.000233	0.625	0.000233
0.609	0.000233	0.609	0.000233	0.791	0.000233	0.625	0.000233
0.609	0.000233	0.609	0.000233	0.774	0.000233	0.625	0.000233
0.609	0.000233	0.609	0.000233	0.774	0.000233	0.625	0.000233
0.609	0.000233	0.609	0.000233	0.741	0.000233	0.625	0.000233
0.592	0.000233	0.609	0.000233	0.692	0.000233	0.625	0.000233
0.592	0.000233	0.609	0.000233	0.642	0.000233	0.625	0.000233
0.592	0.000233	0.592	0.000233	0.592	0.000233	0.592	0.000233
0.559	0.000233	0.559	0.001163	0.559	0.00186	0.559	0.00186
0.51	0.00186	0.493	0.007209	0.493	0.012791	0.493	0.015814
0.443	0.015814	0.443	0.032791	0.443	0.046047	0.443	0.054419
0.394	0.033488	0.394	0.055349	0.394	0.079302	0.394	0.096279
0.344	0.048372	0.344	0.076279	0.344	0.110233	0.344	0.139767
0.294	0.063023	0.294	0.097907	0.294	0.139767	0.294	0.176977
0.245	0.08	0.245	0.121163	0.245	0.168372	0.245	0.211628
0.195	0.097907	0.195	0.145814	0.195	0.197674	0.195	0.245814
0.145	0.115581	0.145	0.17	0.145	0.224884	0.145	0.276047
0.096	0.135116	0.096	0.193953	0.096	0.252791	0.096	0.306279
$T = 70\,°C$		$T = 75\,°C$		$T = 80\,°C$			
V	I (A cm^{-2})	V	I (A cm^{-2})	V	I (A cm^{-2})		
0.658	0.000233	0.658	0.000233	0.609	0.000233		
0.642	0.000233	0.642	0.000233	0.609	0.000233		
0.625	0.000233	0.642	0.000233	0.609	0.000233		
0.625	0.000233	0.625	0.000233	0.609	0.000233		
0.625	0.000233	0.625	0.000233	0.625	0.000233		
0.625	0.000233	0.625	0.000233	0.609	0.000233		
0.625	0.000233	0.625	0.000233	0.609	0.000233		
0.625	0.000233	0.609	0.000233	0.609	0.000233		
0.592	0.000233	0.592	0.000233	0.592	0.000233		
0.559	0.002558	0.559	0.00186	0.559	0.001163		
0.493	0.013488	0.493	0.01186	0.493	0.008837		
0.443	0.055349	0.443	0.051395	0.443	0.044419		
0.394	0.10186	0.394	0.098605	0.394	0.089302		
0.344	0.157442	0.344	0.153721	0.344	0.142093		
0.294	0.209302	0.294	0.209302	0.294	0.198605		
0.245	0.250465	0.245	0.260465	0.245	0.255116		
0.195	0.286047	0.195	0.296047	0.195	0.298372		
0.145	0.315581	0.145	0.324884	0.145	0.330233		
0.096	0.346512	0.096	0.353488	0.096	0.354884		

Methanol concentration, 3 M; cathode humidification temperature, 30 °C; methanol flow rate, 4 ml min^{-1}; air flow rate, 600 sccm.

Table 2
The experimental data of cell performance at different methanol concentrations (air flow rate: 600 sccm)

C = 0.5 M		C = 1 M		C = 2 M		C = 3 M	
V	I (A cm^{-2})	V	I (A cm^{-2})	V	I (A cm^{-2})	V	I (A cm^{-2})
0.824	2E−4	0.774	2E−4	0.791	2E−4	0.725	2E−4
0.807	2E−4	0.774	2E−4	0.774	2E−4	0.692	2E−4
0.791	2E−4	0.774	2E−4	0.758	2E−4	0.692	2E−4
0.791	2E−4	0.774	2E−4	0.758	2E−4	0.675	2E−4
0.791	2E−4	0.774	2E−4	0.758	2E−4	0.675	2E−4
0.741	0.0016	0.741	1E−3	0.741	2E−4	0.675	2E−4
0.692	0.0016	0.692	2E−4	0.692	2E−4	0.675	2E−4
0.642	0.0016	0.642	0.0016	0.642	2E−4	0.642	2E−4
0.592	0.0062	0.592	0.0042	0.592	0.0016	0.592	1E−3
0.559	0.0176	0.559	0.0162	0.559	0.0102	0.559	0.003
0.493	0.0382	0.51	0.0422	0.493	0.0282	0.51	0.0156
0.443	0.0868	0.443	0.0942	0.443	0.0816	0.443	0.0568
0.394	0.125	0.394	0.139	0.394	0.133	0.394	0.1
0.344	0.168	0.344	0.191	0.344	0.186	0.344	0.151
0.294	0.205	0.294	0.243	0.294	0.239	0.294	0.201
0.245	0.232	0.245	0.291	0.245	0.288	0.245	0.239
0.195	0.242	0.195	0.327	0.195	0.324	0.195	0.275
0.145	0.25	0.145	0.357	0.145	0.355	0.162	0.297
0.096	0.252	0.096	0.381	0.096	0.387	0.096	0.325

C = 4 M		C = 5 M		C = 6 M	
V	I (A cm^{-2})	V	I (A cm^{-2})	V	I (A cm^{-2})
0.576	2E−4	0.526	2E−4	0.493	2E−4
0.576	2E−4	0.51	2E−4	0.493	2E−4
0.559	2E−4	0.51	2E−4	0.476	2E−4
0.576	2E−4	0.51	2E−4	0.476	2E−4
0.576	2E−4	0.51	2E−4	0.476	2E−4
0.576	2E−4	0.51	2E−4	0.493	2E−4
0.576	2E−4	0.51	2E−4	0.476	0.0308
0.576	2E−4	0.51	2E−4	0.493	0.0896
0.576	2E−4	0.51	2E−4	0.493	0.148
0.559	1E−3	0.51	2E−4	0.493	0.195
0.493	0.0096	0.493	0.003	0.476	2E−4
0.443	0.0362	0.443	0.0216	0.443	2E−4
0.394	0.0702	0.394	0.0482	0.394	2E−4
0.344	0.11	0.344	0.0816	0.344	2E−4
0.294	0.151	0.294	0.117	0.294	2E−4
0.245	0.186	0.245	0.156	0.245	2E−4
0.195	0.218	0.195	0.182	0.195	0.0308
0.145	0.247	0.145	0.208	0.145	0.0896
0.096	0.266	0.096	0.227	0.096	0.148

Cell temperature, 70 °C; cathode humidification temperature, 70 °C; methanol flow rate, 6 ml min^{-1}; air flow rate, 600 sccm.

Table 3
The experimental data of cell performance at different methanol concentrations (air flow rate 1200 sccm)

C = 0.5 M		C = 1 M		C = 2 M		C = 3 M	
V	I (A cm^{-2})	V	I (A cm^{-2})	V	I (A cm^{-2})	V	I (A cm^{-2})
0.824	2E−4	0.807	2E−4	0.791	2E−4	0.725	2E−4
0.807	2E−4	0.807	2E−4	0.774	2E−4	0.725	2E−4
0.807	2E−4	0.807	2E−4	0.774	2E−4	0.708	2E−4
0.807	2E−4	0.791	2E−4	0.774	2E−4	0.692	2E−4
0.791	2E−4	0.791	2E−4	0.774	2E−4	0.692	2E−4
0.741	1E−3	0.741	1E−3	0.741	2E−4	0.692	2E−4
0.692	0.0016	0.692	1E−3	0.692	2E−4	0.692	2E−4
0.642	0.0016	0.642	0.0016	0.642	1E−3	0.642	2E−4
0.592	0.0056	0.592	0.005	0.592	0.0036	0.592	0.0016
0.559	0.0196	0.559	0.0196	0.559	0.0102	0.559	0.0042
0.51	0.0468	0.493	0.0508	0.493	0.0336	0.493	0.0202

Table 3 (*Continued*)

C = 0.5 M		C = 1 M		C = 2 M		C = 3 M	
V	I (A cm^{-2})	V	I (A cm^{-2})	V	I (A cm^{-2})	V	I (A cm^{-2})
0.443	0.0942	0.443	0.105	0.443	0.0928	0.443	0.0702
0.394	0.137	0.394	0.157	0.394	0.151	0.394	0.123
0.344	0.178	0.344	0.211	0.344	0.209	0.344	0.185
0.294	0.218	0.294	0.267	0.294	0.272	0.294	0.244
0.245	0.235	0.245	0.316	0.245	0.328	0.245	0.301
0.195	0.247	0.195	0.353	0.195	0.383	0.195	0.349
0.145	0.252	0.145	0.377	0.145	0.429	0.145	0.393
0.096	0.253	0.096	0.393	0.096	0.472	0.096	0.432

C = 4 M		C = 5 M		C = 6 M	
V	I (A cm^{-2})	V	I (A cm^{-2})	V	I (A cm^{-2})
0.609	2E−4	0.625	2E−4	0.543	2E−4
0.592	2E−4	0.543	2E−4	0.51	2E−4
0.609	2E−4	0.526	2E−4	0.51	2E−4
0.609	2E−4	0.526	2E−4	0.51	2E−4
0.609	2E−4	0.526	2E−4	0.51	2E−4
0.609	2E−4	0.526	2E−4	0.51	2E−4
0.609	2E−4	0.526	2E−4	0.51	2E−4
0.609	2E−4	0.526	2E−4	0.51	2E−4
0.592	2E−4	0.526	2E−4	0.51	2E−4
0.559	0.0022	0.526	2E−4	0.51	2E−4
0.51	0.0096	0.493	0.0036	0.493	0.0016
0.443	0.0388	0.443	0.0276	0.443	0.021
0.394	0.0782	0.394	0.0656	0.394	0.0488
0.344	0.133	0.344	0.111	0.344	0.0902
0.294	0.192	0.294	0.166	0.294	0.137
0.245	0.249	0.245	0.218	0.245	0.189
0.195	0.299	0.195	0.267	0.195	0.235
0.145	0.342	0.145	0.309	0.145	0.279
0.096	0.386	0.096	0.348	0.096	0.313

Cell temperature, 70 °C; cathode humidification temperature, 70 °C; methanol flow rate, 6 ml min^{-1}; air flow rate, 1200 sccm.

Table 4
The experimental data of cell performance at different methanol concentrations (pure oxygen flow rate 600 sccm)

C = 0.5 M		C = 1 M		C = 2 M		C = 3 M	
V	I (A cm^{-2})	V	I (A cm^{-2})	V	I (A cm^{-2})	V	I (A cm^{-2})
0.824	2E−4	0.841	2E−4	0.824	2E−4	0.841	2E−4
0.824	2E−4	0.841	2E−4	0.824	2E−4	0.824	2E−4
0.824	2E−4	0.841	2E−4	0.824	2E−4	0.824	2E−4
0.824	2E−4	0.841	2E−4	0.807	2E−4	0.807	2E−4
0.791	2E−4	0.791	0.0016	0.791	2E−4	0.791	2E−4
0.741	2E−4	0.741	1E−3	0.741	2E−4	0.741	1E−3
0.692	2E−4	0.692	0.0016	0.692	0.0016	0.692	1E−3
0.642	0.0022	0.642	0.0022	0.642	0.0016	0.642	0.0022
0.592	0.019	0.592	0.009	0.592	0.011	0.592	0.0096
0.559	0.0542	0.559	0.0336	0.559	0.0356	0.559	0.0288
0.51	0.0956	0.51	0.0676	0.493	0.0862	0.51	0.0736
0.443	0.164	0.443	0.138	0.443	0.185	0.443	0.176
0.394	0.22	0.394	0.196	0.394	0.268	0.394	0.269
0.344	0.251	0.344	0.258	0.344	0.357	0.344	0.366
0.294	0.263	0.294	0.306	0.294	0.45	0.294	0.46
0.245	0.267	0.245	0.336	0.245	0.538	0.245	0.56
0.195	0.267	0.195	0.353	0.195	0.628	0.195	0.658
0.145	0.271	0.145	0.363	0.145	0.711	0.145	0.748
0.096	0.269	0.096	0.373	0.096	0.787	0.096	0.839

Table 4 (*Continued*)

$C = 4$ M		$C = 5$ M		$C = 6$ M	
V	I (A cm^{-2})	V	I (A cm^{-2})	V	I (A cm^{-2})
0.774	2E−4	0.791	2E−4	0.791	2E−4
0.774	2E−4	0.774	2E−4	0.774	2E−4
0.758	2E−4	0.758	2E−4	0.741	2E−4
0.758	2E−4	0.758	2E−4	0.725	2E−4
0.741	2E−4	0.741	2E−4	0.708	2E−4
0.741	2E−4	0.725	2E−4	0.692	2E−4
0.692	2E−4	0.692	2E−4	0.692	2E−4
0.642	1E−3	0.642	2E−4	0.642	2E−4
0.592	0.0036	0.592	0.0022	0.592	0.0016
0.559	0.0162	0.559	0.0142	0.559	0.011
0.493	0.0502	0.493	0.0456	0.493	0.0396
0.443	0.143	0.443	0.127	0.443	0.119
0.394	0.233	0.394	0.217	0.394	0.206
0.344	0.335	0.344	0.317	0.344	0.307
0.294	0.435	0.294	0.421	0.294	0.417
0.245	0.529	0.245	0.524	0.245	0.523
0.195	0.627	0.195	0.621	0.195	0.626
0.145	0.718	0.145	0.714	0.145	0.723
0.096	0.808	0.096	0.807	0.096	0.817

Cell temperature, 70 °C; cathode humidification temperature, 70 °C; methanol flow rate, 6 ml min^{-1}; pure oxygen flow rate, 600 sccm.

Table 5
The experimental data of cell performance at different cathode humidification temperatures

$T = 40$ °C		$T = 50$ °C		$T = 60$ °C		$T = 70$ °C	
V	I (A cm^{-2})	V	I (A cm^{-2})	V	I (A cm^{-2})	V	I (A cm^{-2})
0.741	2E−4	0.758	2E−4	0.774	2E−4	0.758	2E−4
0.675	2E−4	0.725	2E−4	0.741	2E−4	0.658	2E−4
0.625	2E−4	0.642	2E−4	0.658	2E−4	0.609	2E−4
0.642	2E−4	0.609	2E−4	0.625	2E−4	0.592	2E−4
0.692	2E−4	0.592	2E−4	0.625	2E−4	0.576	2E−4
0.725	2E−4	0.625	2E−4	0.609	2E−4	0.576	2E−4
0.692	2E−4	0.658	2E−4	0.642	2E−4	0.576	2E−4
0.642	1E−3	0.642	2E−4	0.642	2E−4	0.576	2E−4
0.592	1E−3	0.592	1E−3	0.592	0.0022	0.592	2E−4
0.559	0.0062	0.559	0.005	0.559	0.007	0.559	0.0042
0.493	0.025	0.493	0.0202	0.51	0.023	0.493	0.017
0.443	0.0708	0.443	0.0642	0.443	0.0688	0.443	0.0582
0.394	0.111	0.394	0.106	0.394	0.115	0.394	0.104
0.344	0.163	0.344	0.155	0.344	0.163	0.344	0.15
0.294	0.209	0.294	0.206	0.294	0.207	0.294	0.195
0.245	0.251	0.245	0.253	0.245	0.251	0.245	0.237
0.195	0.288	0.195	0.293	0.195	0.288	0.195	0.275
0.145	0.32	0.145	0.327	0.145	0.317	0.145	0.309
0.096	0.345	0.096	0.359	0.096	0.345	0.096	0.343
$T = 80$ °C		$T = 90$ °C					
V	I (A cm^{-2})	V	I (A cm^{-2})				
0.725	2E−4	0.692	2E−4				
0.625	2E−4	0.609	2E−4				
0.609	2E−4	0.592	2E−4				
0.609	2E−4	0.592	2E−4				
0.592	2E−4	0.592	2E−4				
0.592	2E−4	0.592	0.0202				
0.609	2E−4	0.592	0.101				
0.609	2E−4	0.592	0.186				
0.609	2E−4	0.592	0.262				
0.559	0.007	0.559	0.328				

Table 5 (*Continued*)

T = 80 °C		*T* = 90 °C	
V	*I* (A cm^{-2})	*V*	*I* (A cm^{-2})
0.493	0.0216	0.51	2E−4
0.443	0.0668	0.443	2E−4
0.394	0.107	0.394	2E−4
0.344	0.154	0.344	2E−4
0.294	0.196	0.294	2E−4
0.245	0.236	0.245	0.0202
0.195	0.273	0.195	0.101
0.145	0.305	0.145	0.186
0.096	0.335	0.096	0.262

Air flow rate, 600 sccm; cell temperature, 70 °C; methanol concentration, 2 M; methanol flow rate, 6 ml min^{-1}; air flow rate, 600 sccm.

Table 6
The experimental data of cell performance at different cathode humidification temperatures

T = 40 °C		*T* = 50 °C		*T* = 60 °C		*T* = 70 °C	
V	*I* (A cm^{-2})	*V*	*I* (A cm^{-2})	*V*	*I* (A cm^{-2})	*V*	*I* (A cm^{-2})
0.774	2E−4	0.758	2E−4	0.758	2E−4	0.741	2E−4
0.758	2E−4	0.741	2E−4	0.725	2E−4	0.642	2E−4
0.758	2E−4	0.725	2E−4	0.692	2E−4	0.609	2E−4
0.758	2E−4	0.741	2E−4	0.658	2E−4	0.625	2E−4
0.758	2E−4	0.741	2E−4	0.725	2E−4	0.741	2E−4
0.741	2E−4	0.741	2E−4	0.725	2E−4	0.741	2E−4
0.692	2E−4	0.692	1E−3	0.692	2E−4	0.692	2E−4
0.642	1E−3	0.642	1E−3	0.642	2E−4	0.642	1E−3
0.592	0.0022	0.592	0.0022	0.592	0.0016	0.592	1E−3
0.559	0.0102	0.559	0.009	0.559	0.007	0.559	0.0062
0.51	0.0262	0.493	0.0256	0.493	0.0282	0.493	0.0262
0.443	0.0828	0.443	0.0782	0.443	0.0756	0.443	0.0748
0.394	0.13	0.394	0.129	0.394	0.127	0.394	0.121
0.344	0.186	0.344	0.182	0.344	0.18	0.344	0.174
0.294	0.245	0.294	0.24	0.294	0.232	0.294	0.225
0.245	0.303	0.245	0.293	0.245	0.285	0.245	0.278
0.195	0.353	0.195	0.346	0.195	0.333	0.195	0.322
0.145	0.401	0.145	0.391	0.145	0.376	0.145	0.368
0.096	0.442	0.096	0.433	0.096	0.414	0.096	0.407
T = 80 °C		*T* = 90 °C					
V	*I* (A cm^{-2})	*V*	*I* (A cm^{-2})				
0.791	2E−4	0.741	2E−4				
0.741	2E−4	0.625	2E−4				
0.658	2E−4	0.592	2E−4				
0.625	2E−4	0.592	2E−4				
0.609	2E−4	0.592	2E−4				
0.609	2E−4	0.592	2E−4				
0.609	2E−4	0.592	2E−4				
0.592	2E−4	0.592	2E−4				
0.592	2E−4	0.592	2E−4				
0.559	0.0082	0.559	0.0042				
0.493	0.027	0.493	0.021				
0.443	0.0742	0.443	0.0656				
0.394	0.121	0.394	0.11				
0.344	0.173	0.344	0.161				
0.294	0.223	0.294	0.209				
0.245	0.271	0.245	0.258				
0.195	0.321	0.195	0.305				
0.145	0.361	0.145	0.348				
0.096	0.403	0.096	0.389				

Air flow rate, 1200 sccm; cell temperature, 70 °C; methanol concentration, 2 M; methanol flow rate, 6 ml min^{-1}; air flow rate, 1200 sccm.

Table 7
The experimental data of cell performance at different methanol flow rates

0.5 ml min^{-1}		1.0 ml min^{-1}		2.0 ml min^{-1}		3.0 ml min^{-1}		4.0 ml min^{-1}	
V	*I* (A cm^{-2})	*V*	*I* (A cm^{-2})	*V*	*I* (A cm^{-2})	*V*	*I* (A cm^{-2})	*V*	*I* (A cm^{-2})
0.774	2E−4	0.824	2E−4	0.807	2E−4	0.807	2E−4	0.807	2E−4
0.807	2E−4	0.807	2E−4	0.807	2E−4	0.791	2E−4	0.791	2E−4
0.807	2E−4	0.807	2E−4	0.791	2E−4	0.774	2E−4	0.758	2E−4
0.807	2E−4	0.791	2E−4	0.774	2E−4	0.758	2E−4	0.741	2E−4
0.791	2E−4	0.774	2E−4	0.758	2E−4	0.741	2E−4	0.725	2E−4
0.741	1E−3	0.741	2E−4	0.741	2E−4	0.725	2E−4	0.708	2E−4
0.692	0.0022	0.692	1E−3	0.692	0.0016	0.692	2E−4	0.692	2E−4
0.642	0.0036	0.642	0.0016	0.642	1E−3	0.642	0.0022	0.642	1E−3
0.592	0.007	0.592	0.0062	0.592	0.0056	0.592	0.0036	0.592	0.005
0.559	0.0162	0.559	0.0176	0.559	0.0182	0.559	0.0122	0.559	0.015
0.493	0.0316	0.493	0.0388	0.493	0.0362	0.493	0.0368	0.493	0.0336
0.443	0.0602	0.443	0.0702	0.443	0.0796	0.443	0.0768	0.443	0.0802
0.394	0.0888	0.394	0.103	0.394	0.116	0.394	0.114	0.394	0.115
0.344	0.103	0.344	0.131	0.344	0.157	0.344	0.157	0.344	0.159
0.294	0.103	0.294	0.149	0.294	0.195	0.294	0.202	0.294	0.203
0.245	0.0942	0.245	0.155	0.245	0.221	0.245	0.231	0.245	0.24
0.195	0.0936	0.195	0.156	0.195	0.228	0.195	0.254	0.195	0.263
0.145	0.0868	0.145	0.153	0.145	0.228	0.145	0.257	0.145	0.28
0.096	0.0836	0.096	0.145	0.096	0.223	0.096	0.262	0.096	0.285

5.0 ml min^{-1}		7.0 ml min^{-1}		8.0 ml min^{-1}		10.0 ml min^{-1}	
V	*I* (A cm^{-2})	*V*	*I* (A cm^{-2})	*V*	*I* (A cm^{-2})	*V*	*I* (A cm^{-2})
0.791	2E−4	0.791	2E−4	0.791	2E−4	0.774	2E−4
0.774	2E−4	0.758	2E−4	0.758	2E−4	0.741	2E−4
0.758	2E−4	0.741	2E−4	0.741	2E−4	0.725	2E−4
0.725	2E−4	0.708	2E−4	0.708	2E−4	0.708	2E−4
0.708	2E−4	0.692	2E−4	0.692	2E−4	0.675	2E−4
0.692	2E−4	0.658	2E−4	0.675	2E−4	0.658	2E−4
0.658	2E−4	0.642	2E−4	0.675	2E−4	0.658	2E−4
0.642	0.0016	0.642	2E−4	0.642	1E−3	0.642	2E−4
0.592	0.003	0.592	0.003	0.592	0.005	0.592	0.0022
0.559	0.0116	0.559	0.0142	0.559	0.0116	0.559	0.0096
0.493	0.0316	0.493	0.0316	0.493	0.0322	0.493	0.0316
0.443	0.0782	0.443	0.0762	0.443	0.0776	0.443	0.0736
0.394	0.111	0.394	0.113	0.394	0.116	0.394	0.109
0.344	0.159	0.344	0.153	0.344	0.155	0.344	0.153
0.294	0.199	0.294	0.195	0.294	0.201	0.294	0.197
0.245	0.237	0.245	0.239	0.245	0.243	0.245	0.238
0.195	0.267	0.195	0.275	0.195	0.278	0.195	0.275
0.145	0.288	0.145	0.295	0.145	0.303	0.145	0.302
0.096	0.3	0.096	0.312	0.096	0.32	0.096	0.323

Air flow rate, 1200 sccm; cell temperature, 70 °C; cathode humidification temperature, 70 °C; methanol concentration, 1 M; air flow rate, 1200 sccm.

Table 8
The experimental data of cell performance at different methanol flow rates

0.5 ml min^{-1}		1.0 ml min^{-1}		3.0 ml min^{-1}		5.0 ml min^{-1}	
V	*I* (A cm^{-2})	*V*	*I* (A cm^{-2})	*V*	*I* (A cm^{-2})	*V*	*I* (A cm^{-2})
0.758	2E−4	0.824	2E−4	0.807	2E−4	0.791	2E−4
0.791	2E−4	0.807	2E−4	0.791	2E−4	0.774	2E−4
0.807	2E−4	0.791	2E−4	0.774	2E−4	0.741	2E−4
0.791	2E−4	0.774	2E−4	0.758	2E−4	0.725	2E−4
0.791	2E−4	0.758	2E−4	0.741	2E−4	0.708	2E−4
0.741	1E−3	0.741	2E−4	0.725	2E−4	0.675	2E−4
0.692	0.0016	0.692	2E−4	0.692	0.0016	0.658	2E−4
0.642	0.003	0.642	0.003	0.642	0.0016	0.642	2E−4
0.592	0.0096	0.592	0.007	0.592	0.005	0.592	0.0022
0.559	0.017	0.559	0.015	0.559	0.015	0.559	0.0136
0.493	0.0296	0.493	0.0348	0.493	0.0336	0.51	0.0302

Table 8 (*Continued*)

0.5 ml min^{-1}		1.0 ml min^{-1}		3.0 ml min^{-1}		5.0 ml min^{-1}	
V	*I* (A cm^{-2})	*V*	*I* (A cm^{-2})	*V*	*I* (A cm^{-2})	*V*	*I* (A cm^{-2})
0.443	0.0568	0.443	0.0708	0.443	0.0708	0.443	0.0736
0.394	0.0856	0.394	0.101	0.394	0.107	0.394	0.107
0.344	0.0962	0.344	0.133	0.344	0.147	0.344	0.148
0.294	0.1	0.294	0.157	0.294	0.185	0.294	0.188
0.245	0.0974	0.245	0.166	0.245	0.223	0.245	0.222
0.195	0.0896	0.195	0.165	0.195	0.241	0.195	0.254
0.145	0.0848	0.145	0.163	0.145	0.248	0.145	0.272
0.096	0.0828	0.096	0.159	0.096	0.253	0.096	0.284
8.0 ml min^{-1}		10.0 ml min^{-1}					
V	*I* (A cm^{-2})	*V*	*I* (A cm^{-2})				
0.791	2E−4	0.774	2E−4				
0.758	2E−4	0.741	2E−4				
0.741	2E−4	0.708	2E−4				
0.725	2E−4	0.692	2E−4				
0.708	2E−4	0.658	2E−4				
0.675	2E−4	0.658	2E−4				
0.692	2E−4	0.642	2E−4				
0.642	0.0016	0.658	2E−4				
0.592	0.0042	0.592	0.0036				
0.559	0.0122	0.559	0.0102				
0.493	0.0288	0.493	0.0296				
0.443	0.0728	0.443	0.0696				
0.394	0.105	0.394	0.103				
0.344	0.146	0.344	0.143				
0.294	0.189	0.294	0.185				
0.245	0.222	0.245	0.223				
0.195	0.254	0.195	0.254				
0.145	0.281	0.145	0.283				
0.096	0.303	0.096	0.305				

Air flow rate, 600 sccm; cell temperature, 70 °C; cathode humidification temperature, 70 °C; methanol concentration, 1 M; air flow rate, 600 sccm.

Table 9
The experimental data of cell performance at different air flow rates

Different air flow rate (sccm)							
300		500		800		1000	
V	*I* (A cm^{-2})	*V*	*I* (A cm^{-2})	*V*	*I* (A cm^{-2})	*V*	*I* (A cm^{-2})
(a) Methanol concentration: 2 M							
0.625	2.32558E−4	0.708	2.32558E−4	0.725	2.32558E−4	0.708	2.32558E−4
0.609	2.32558E−4	0.692	2.32558E−4	0.692	2.32558E−4	0.675	2.32558E−4
0.609	2.32558E−4	0.692	2.32558E−4	0.675	2.32558E−4	0.675	2.32558E−4
0.609	2.32558E−4	0.692	2.32558E−4	0.675	2.32558E−4	0.658	2.32558E−4
0.609	2.32558E−4	0.692	2.32558E−4	0.658	2.32558E−4	0.658	2.32558E−4
0.609	2.32558E−4	0.675	2.32558E−4	0.658	2.32558E−4	0.658	2.32558E−4
0.625	2.32558E−4	0.675	2.32558E−4	0.642	2.32558E−4	0.658	2.32558E−4
0.609	2.32558E−4	0.642	2.32558E−4	0.642	2.32558E−4	0.642	2.32558E−4
0.592	0.00116	0.592	0.00116	0.592	0.00186	0.592	0.00186
0.559	0.00651	0.559	0.00884	0.559	0.01047	0.559	0.01116
0.493	0.02349	0.493	0.02744	0.493	0.03279	0.493	0.03581
0.443	0.07	0.443	0.08093	0.443	0.09023	0.443	0.09791
0.394	0.11488	0.394	0.13186	0.394	0.14442	0.394	0.15209
0.344	0.1514	0.344	0.17605	0.344	0.1893	0.344	0.19628
0.294	0.17698	0.294	0.21023	0.294	0.22488	0.294	0.23186
0.245	0.20093	0.245	0.24047	0.245	0.25814	0.245	0.26442
0.195	0.21628	0.195	0.26977	0.195	0.28674	0.195	0.29535
0.145	0.23419	0.145	0.29372	0.145	0.31465	0.145	0.32256
0.096	0.24651	0.096	0.31558	0.096	0.34023	0.096	0.34721

Table 9 (*Continued*)

Different air flow rate (sccm)							
100		600		1600		2000	
V	*I* (A cm^{-2})	*V*	*I* (A cm^{-2})	*V*	*I* (A cm^{-2})	*V*	*I* (A cm^{-2})
(b) Methanol concentration: 4 M							
0.394	2.32558E−4	0.526	2.32558E−4	0.741	2.32558E−4	0.708	2.32558E−4
0.377	2.32558E−4	0.526	2.32558E−4	0.725	2.32558E−4	0.708	2.32558E−4
0.394	2.32558E−4	0.526	2.32558E−4	0.708	2.32558E−4	0.692	2.32558E−4
0.377	2.32558E−4	0.543	2.32558E−4	0.708	2.32558E−4	0.675	2.32558E−4
0.394	2.32558E−4	0.543	2.32558E−4	0.692	2.32558E−4	0.658	2.32558E−4
0.394	2.32558E−4	0.543	2.32558E−4	0.675	2.32558E−4	0.642	2.32558E−4
0.394	2.32558E−4	0.543	2.32558E−4	0.658	2.32558E−4	0.625	2.32558E−4
0.394	2.32558E−4	0.543	2.32558E−4	0.642	2.32558E−4	0.609	2.32558E−4
0.394	2.32558E−4	0.543	2.32558E−4	0.592	2.32558E−4	0.592	2.32558E−4
0.394	2.32558E−4	0.543	2.32558E−4	0.559	0.00186	0.559	0.00116
0.394	2.32558E−4	0.493	0.00953	0.493	0.00953	0.493	0.00651
0.377	2.32558E−4	0.443	0.04512	0.443	0.05372	0.443	0.03977
0.394	2.32558E−4	0.394	0.08628	0.394	0.11256	0.394	0.09093
0.344	0.00581	0.344	0.13186	0.344	0.18395	0.344	0.15977
0.294	0.01419	0.294	0.17837	0.294	0.26047	0.294	0.23814
0.245	0.01977	0.245	0.21488	0.245	0.33488	0.245	0.32023
0.195	0.02116	0.195	0.24651	0.195	0.39535	0.195	0.39605
0.145	0.02744	0.145	0.26837	0.145	0.44093	0.145	0.45488
0.096	0.03442	0.096	0.29233	0.096	0.47419	0.096	0.49674

Methanol concentrations, 2 M (a) and 4 M (b); cell temperature, 75 °C; cathode humidification temperature, 75 °C; methanol flow rates, 5 ml min^{-1} (a) and 4 ml min^{-1} (b).

References

[1] S. Surampidi, S.R. Narayanan, E. Vamos, H. Frank, G. Halpert, A. LaConti, J. Kosek, G.K. Surya Prakash, G.A. Olah, Advances in direct oxidation methanol fuel cells, J. Power Sources 47 (1994) 377–385.

[2] D.H. Jung, C.H. Lee, C.S. Kim, D.R. Shin, Performance of a direct methanol polymer electrolyte fuel cell, J. Power Sources 71 (1998) 169–173.

[3] N. Nakagawa, Y. Xiu, Performance of a direct methanol fuel cell operated at atmospheric pressure, J. Power Sources 118 (2003) 248–255.

[4] S.R. Narayanan, A. Kindle, B. Jeffries-Nakamura, W. Chun, H. Frank, M. Smart, T.I. Valdez, S. Surampudi, G. Halpert, J. Kosek, C. Cropley:, Recent advances in PEM liquid-feed direct methanol fuel cells, Ann. Battery Conf. Appl. Adv. 11 (1996) 113.

[5] T.I. Valdez, S.R. Narayanan, Recent studies on methanol crossover in liquid-feed direct methanol fuel cells, Proceedings of the 194th Meeting of the Electrochemical Society, Boston, November 1998.

[6] H. Dohle, J. Divisek, R. Jung, Process engineering of the direct methanol fuel cell, J. Power Sources 86 (2000) 469–477.

[7] A.K. Shukla, P.A. Christensen, A.J. Dickinson, A. Hamnett:, A liquid-feed solid polymer electrolyte direct methanol fuel cell operating at near ambient conditions, J. Power Sources 76 (1998) 54–59.

[8] A.K. Shukla, C.L. Jackson, K. Scott, G. Murgia, A solid-polymer electrolyte direct methanol fuel cell with a mixed reactant and air anode, J. Power Sources 111 (2002) 43–51.

[9] H. Dohle, H. Schmitz, T. Bewer, J. Mergel, D. Stolten, Development of a compact 500W class direct methanol fuel cell stack, J. Power Sources 106 (2002) 313–322.